ACS APPLIED MATERIALS & INTERFACES

Research Article

www.acsami.org

Mechanical, In vitro Antimicrobial, and Biological Properties of Plasma-Sprayed Silver-Doped Hydroxyapatite Coating

Mangal Roy,[†] Gary A. Fielding,[†] Haluk Beyenal,[‡] Amit Bandyopadhyay,[†] and Susmita Bose*[,†]

[†]W. M. Keck Biomedical Materials Research Laboratory School of Mechanical and Materials Engineering [‡]Gene and Linda Voiland School of Chemical Engineering and Bioengineering, Washington State University, Pullman, Washington 99164, United States

ABSTRACT: Implant-related infection is one of the key concerns in total joint hip arthroplasties. To reduce bacterial adhesion, we used silver (Ag)/silver oxide (Ag_2O) doping in plasma sprayed hydroxyapatite (HA) coating on titanium substrate. HA powder was doped with 2.0, 4.0, and 6.0 wt % Ag, heat-treated at 800 °C and used for plasma spray coating using a 30 kW plasma spray system, equipped with supersonic nozzle. Application of supersonic plasma nozzle significantly reduced phase decomposition and amorphous phase formation in the HA coatings as evident by X-ray diffraction (XRD) study and Fourier transformed infrared spectroscopic (FTIR) analysis. Adhesive bond strength of more than 15 MPa ensured the mechanical integrity of the coatings. Resistance against bacterial adhesion of the coatings was determined by challenging them against *Pseudomonas aeruginosa* (PAO1). Live/dead staining of the adherent bacteria on the coating surfaces indicated a significant reduction in bacterial adhesion due to the presence of Ag. In vitro cell-material interactions and alkaline phosphatase (ALP) protein expressions were evaluated by culturing human fetal osteoblast cells (hFOB). Our results suggest that the plasma-sprayed HA coatings doped with an optimum amount of Ag can have excellent antimicrobial property without altering mechanical property of the Ag-doped HA coatings.

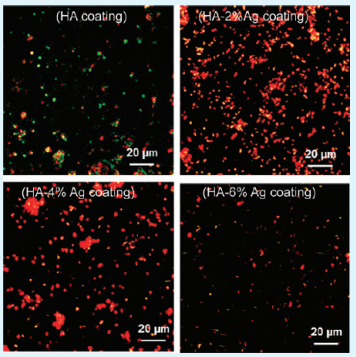

KEYWORDS: *HA coating, plasma spray, Pseudomonas aeruginosa, biocompatibility*

1. INTRODUCTION

In recent years, hydroxyapatite (HA) has been used as coatings in load-bearing metallic implants because of its osteoconductivity and chemical similarity to bone. Different coating technologies have been developed over the years, among which plasma spray is the only commercial coating technique.[1−5] Certain advantages of plasma spray such as ease of operation, low cost, and bulk production made this process of commercial choice over other techniques. However, the issues associated with plasma spray are phase decomposition and amorphous phase formation, which needs to be addressed considering the long-term stability and performance of HA coatings.[6]

Clinical successes of HA coated metallic implants are well-documented. At early stage of implantation (up to 5 years), HA coatings showed better performance than uncoated implants in terms of osseous ingrowth, fewer loosening followed by revisions.[7−9] Long-term clinical follow up (up to 13 years) studies indicated reliable and promising results for HA coated metallic implants.[10,11] However, the most promising results of HA-coated metallic implants were found in revision hip surgeries.[12,13] The revision hip surgery is primarily done for femoral component and/or acetabular cup. Femoral revision with extensively HA-coated femoral components showed excellent results in short-term revision.[12,13] Long-term clinical and radiological performance was excellent for fully HA-coated femoral component.[13,14] In spite of the good performance of HA coatings in revision surgery, overall performances of revision prosthesis have inferior results than primary.[15] One of the reasons of implant failure is bacterial infection. Despite strict operative procedures such as ultraclean air, laminar airflow, prophylactic antibiotics, and whole-body exhaust ventilated suits, 0.5−3.0% primary and up to 8% revision implants have failed in total hip arthoplasty.[16,17] Compared to a survival rate of 98.1% for aseptic loosening of HA-coated cups for acetabular revision, 90.8% success rate has been reported (mean follow-up of 7.6 years) for nonaseptic loosening.[18] It has also been found that patients with infected prosthesis have to stay in hospital for over 2 times longer than without any infection which can significantly increase (nearly 3 times) the overall cost.[17] Moreover, for open wounds, if biofilm formation happens, surgical removal of implants may be the only option. Therefore, infection-related implant failures are of significant concern and needs to be addressed in order to improve patient's comfort and reduce cost.

Total hip arthoplsaty (THA)-related bacterial infections have been classified in four stages:[19,20] acute infections within the first six weeks (stage I), delayed chronic infections (stage II), infections in already implanted and well-functioned prosthesis (stage III), and unexpected finding of bacterial infections, which was considered as aseptic loosening. Therefore, it is not only important to prevent initial bacterial adhesion on the joint replacements, but also prolonged or sustained antimicrobial

Received: November 17, 2011
Accepted: February 7, 2012
Published: February 7, 2012

activity.[21] To reduce infection in total hip replacement, several researchers have used different antimicrobial agent such as silver (Ag),[22−24] platinum (Pt),[25] vancomycin,[26] gentamycin,[27] ampicillin,[28] and doxycycline.[29] It has generally been accepted that preventing the bacterial adhesion is better than treating the already formed biofilm. Biofilms are highly resistant to external treatment and in often cases removal of the prosthesis become necessity. Among the antimicrobial agents, Ag is a well-known bactericide effective over a wide range of bacteria including antibiotic-resistant bacteria.[22,23] There is also less chance of developing Ag-resistant bacteria in the future which extends its antibacterial efficacy over a period of time.[22] The minimum inhibitory concentrations (MIC) and minimum bactericidal concentration (MBC) of Ag against multidrug-resistant bacteria is 0.78−6.25 μg/mL and 12.5 μg/mL, respectively.[30] In spite of all the advantages, some studies have shown cytotoxic effects of excessive Ag to the mammalian cells.[22,31−33] Therefore, an optimum quantity of Ag on biomedical implants has to be incorporated in order to have good antimicrobial activity with noncytotoxic effects.

In our previous work, we have shown that the presence of Ag on laser-processed tricalcium phosphate coatings can significantly reduce the activity of *P. aeruginosa* and *Staphylococcus aureus*.[32] Several other works have reported successful incorporation of Ag on calcium phosphates and coatings.[26,33] However, the delayed infections for open wounds (stage II or III) can only be prevented if the coatings have a continued resistance against bacterial film formation. For this reason, it is important to incorporate Ag within the HA coating rather than at the HA coating surface. The objective of the present study is to incorporate an optimum amount of Ag in plasma-sprayed HA coating for improved antimicrobial activity without affecting cell−material interactions. The Ag-doped HA coatings were prepared using a 30 kW inductively coupled RF induction plasma spray equipped with supersonic plasma nozzle. The coatings were characterized for phase purity and mechanical stability. Antimicrobial efficacy of the HA and Ag-doped HA coatings were determined against *P. aeruginosa* (PAO1) biofilm formation. This study also investigates the cytocompatibility of the coatings using human fetal osteoblast cells (hFOB).

2. EXPERIMENTAL SECTION

2.1. Coating Preparation. Two-millimeter-thick grade 2 commercially pure titanium substrates (President Titanium, MA) were coated with HA powder with particle size of 150−212 μm. Before coating, the substrate was sandblasted and ultrasonically cleaned in deionized water. The samples were then treated with acetone to remove any remaining organic material. Four compositions of HA were used in the present study: HA, HA-doped with 2.0, 4.0, and 6.0 wt % Ag. Doped powders were prepared by mixing HA and silver oxide (Ag_2O) in a 250 mL of polypropylene bottle containing 75 mL of anhydrous ethanol and 100 g of 5 mm diameter zirconia milling media.[34] The slurries were then ball-milled for 6 h at 70 rpm followed by drying in an oven at 60 °C for 72 h. Ball-milled powder was granulated by heat treatment at 800 °C for 6 h in order to retain particle size distribution of precursor powder.

Coating was performed with a 30 kW inductively coupled radio frequency (RF) plasma spray system (Tekna Plasma Systems, Canada), equipped with axial powder feeding system. From now onward, 2.0, 4.0, and 6.0 wt % Ag-doped HA coatings will be named as HA, HA-2Ag, HA-4Ag, and HA-6Ag, respectively. Working parameters for this study were 25 kW plate power and 110 mm working distance with a supersonic plasma nozzle. Argon (Ar) was used as the central, and carrier gas with flow rate of 25 and 10 standard liters per minute (slpm). A mixture of 60 slpm Ar and 6 slpm hydrogen (H_2) were used as sheath gas. The chamber pressure was maintained at 5 pound-force per square inch gauge (psig). The parameters were selected from previous optimization study where details of the supersonic plasma nozzle were explained.[34,35] By using a supersonic plasma nozzle, HA particles are introduced at a velocity of 510 m/s in the lower region of the plasma torch. The supersonic plasma nozzle results in a particle residence time of 290 μs. A conventional nozzle would have a residence time of 5 ms. The result of using a supersonic plasma nozzle is reduced heat treatment of HA particles.

2.2. Phase Analysis. Phase analysis was performed using a Siemens D500 Krystalloflex X-ray diffractometer using Cu Kα radiation at 35 kV and 30 mA at room temperature. The machine was equipped with a Ni-filter and samples were evaluated over the 2θ range between 20° and 45°, at a step size of 0.02° and a count time of 0.5 s per step. Attenuated total reflection infrared (ATR-IR) was performed to characterize the functional groups present in the coating as well as to assess the crystallinity of the coating. The coatings were scraped off from the substrate and grounded for analysis. The ATR-IR spectra were recorded on a FTIR spectrometer (FTIR, Nicolet 6700, ThermoFisher, Madison, WI) using an ATR diamond crystal and spectra were evaluated between wave numbers of 400 to 4000 cm^{-1}.

2.3. Mechanical Properties. The adhesive strength of the coating to the samples were evaluated using a standard tensile adhesion test (ASTM C633). Testing was performed on 5 replicates.[34] A quick set epoxy resin was used to glue a sandblasted counter Ti substrate to the surface of the HA coating. The samples were cured in an oven at 120 °C for 2 h and then fixtures were subjected to a tensile test at a constant cross head speed of 0.0013 cm/s until failure. Bond strength was calculated as: failure load/sample area (A = 5.06 cm^2). The data were reported as mean ± standard deviation.

2.4. Silver Release. Samples were submersed in phosphate buffered saline (PBS) at pH 7.4[23] and placed on an orbital shaker at 150 rpm in an oven maintained at 36.5 ± 0.5 °C. At each time point, 3 mL of media was collected. After collection, the dissolution tubes were refilled with PBS. The media was analyzed for Ag/Ag^+ concentration using a Shimadzu AA-6800 Atomic Absorption Spectrophotometer (Shimadzu, Kyoto, Japan). Ag^+ standard was purchased from High-Purity Standards (Charleston, SC, USA). Cumulative Ag^+ release is reported in the present work. The % of total Ag released was also calculated based on the amount of Ag present in the respective coatings. Data are presented as mean ± standard deviation

2.5. In vitro Bone Cell−Materials Interaction. Samples were sterilized by autoclaving at 121 °C for 20 min. Established human osteoblast cells hFOB 1.19 (ATCC, Manassas, VA) were seeded onto the samples in equal concentrations and samples were placed in 24-well plates. The cell media used was a 1:1 mixture of Ham's F12 Medium and Dulbecco's Modified Eagle's Medium (DMEM/F12, Sigma, St. Louis, MO), with 2.5 mM L-glutamine (without phenol red). The medium was supplemented with 10% fetal bovine serum (HyClone, Logan, UT) and 0.3 mg/mL G418 (Sigma, St. Louis, MO). Cultures were maintained at 34 °C under an atmosphere of 5% CO_2 as recommended by ATCC for this particular cell line. Medium was changed every 2 days for the duration of the experiment.[3,5]

2.5.1. Cell Morphology. To examine cell morphology, we removed samples from the cell media after 3 days and were fixed with 2% paraformaldehyde/2% glutaraldehyde in 0.1 M cacodylate buffer overnight at 4 °C. After fixation, samples were treated with 2% osmium tetroxide (OsO_4) for 2 h at room temperature. The samples were then dehydrated in an ethanol series (30, 50, 70, 95, and 100% three times), followed by a hexamethyldisilane (HMDS) drying procedure. After gold coating, the samples were observed under field-emission scanning electron microscope (FESEM) (FEI 200F, FEI Inc., OR, USA).[5]

2.5.2. MTT Assay. 3-(4,5-Dimethylthiazol-2-yl)-2,5-diphenyl tetrazolium bromide (MTT) assay was used to evaluate cell viability. The MTT (Sigma, St. Louis, MO) solution was prepared by dissolving MTT in sterile filtered PBS at a concentration of 5 mg/mL. 10% MTT solution was then added to each sample in 24-well plates. After 2 h of incubation, 1 mL of solubilization solution made up of 10% Triton

X-100, 0.1N HCl, and isopropanol was added to dissolve the formazan crystals. One-hundred microliters of the resulting supernatant was transferred into a 96-well plate, and read by a plate reader at 570 nm. Statistical analysis was performed using one way ANOVA, with $p < 0.05$ considered statistically significant. All samples were analyzed in triplicate to ensure reproducibility. Data are presented as mean ± standard deviation.[3,32]

2.5.3. Immunohistochemistry and Confocal Scanning Laser Microscope Imaging. After 5 days and 11 days, samples were removed from cell media and were fixed in 3.7% paraformaldehyde/phosphate buffered solution, pH 7.4 and at room temperature for 10 min. Samples were then washed with PBS for 3 times (5 min each) and permeabilized with 0.1% Triton X-100 (in PBS) for 4 min at room temperature. After permeabilization, samples were washed with TBST and incubated in TBST-BSA (Tris-buffered saline with 1% bovine serum albumin, 250 mM NaCl, pH 8.3) blocking solution for 1 h at room temperature. Primary antibody against alkaline phosphate (ALP) (Sigma, St. Louis, MO) was added at a 1:100 dilution and incubated at 4 °C overnight. Samples were then washed with TBST for 10 min @ 3 times. The secondary antibody, goat antimouse (GAM) Oregon green (Molecular Probes, Eugene, OR), was diluted 1:100 in TBST and added to the samples and incubated for 1 h at room temperature. Samples were then washed with TBST twice (5 min each) followed by 5 min washing with PBS. The samples were mounted on glass coverslips with Vectashield mounting medium (Vector Laboratories, Burlingame, CA) with propidium iodide (PI) and kept at 4 °C for future confocal laser scanning microscope (CLSM) (LSM 510 META, Carl Zeiss MicroImaging, Inc., NY, USA) imaging.

2.6. Antimicrobial Activity. Antimicrobial activity of Ag-doped HA coated samples was determined by challenging with *P. aeruginosa* (PAO1) using a CDC biofilm reactor (Bio Surface Technologies Corporation). The samples were inserted to the holders and the reactor assembly was autoclaved at 121 °C for 20 min. The reactor was initially filled with growth medium and then inoculated. We followed the protocols established in our laboratories[36] for the inoculation and operation of the reactor. A frozen stock of *P. aeruginosa* (PAO1) was inoculated into separate flasks and the cultures were grown for 24 h in 100 mL of tryptic soy broth (TSB) on a shaker set to 150 rpm at room temperature (approximately 25 °C). Before inoculation, the bacterial cell density was quantified by optical methods at 530 nm. After inoculation, the cell density was approximately 1×10^5 cells/mL. The reactor was kept at 37 °C with constant stirring. After 24 h, coupons were taken out of the bioreactor and gently rinsed with PBS. We used a Live/Dead BacLight Bacterial Viability Kit (Molecular Probes Inc., Eugene, OR, USA) to determine the viability of *P. aeruginosa* (PAO1) in biofilms according to the differential cellular uptake of two different stains. The Live/Dead BacLight Bacterial Viability Kit contains two separate solid dyes (components A (SYTO 9) and B (propidium iodide)). A dye solution was prepared by dissolving the contents of components A and B in separate vials containing 2.5 mL of filter-sterilized deionized water (2X solution). These separate solutions were blended (1:1) and used for biofilm staining. The final concentration of the dye solution was 6 μM SYTO 9 stain and 30 μM propidium iodide. Biofilm samples were placed in a sterile Petri plate and stained immediately by adding ~200 μL of stain onto the biofilm surface. The stain was added gently to the edge of the top surface without disturbing the biofilm. The Petri plate was then covered with a cover dish and incubated for 15 min at room temperature to obtain the desired staining in the absence of light. At the end of the staining time, the biofilm sample was rinsed gently with filtered 0.9% NaCl to remove excess stain. Finally, the biofilms were kept in Petri plates containing 0.9% NaCl to protect cell integrity until the CLSM study. The stained biofilms were imaged using a CSLM (LSM 510 META, Carl Zeiss MicroImaging, Inc., NY, USA).

3. RESULTS

3.1. Physicochemical Analysis. X-ray diffraction patterns of the HA and Ag-doped HA coatings are shown in Figure 1. HA (JCPDS no. 09−0432) was found to be the major phase in all of the coatings. Sharp and intense HA peaks at $2\theta = 25.8$ and 32° were clearly visible. Small secondary phases, such as alpha-tricalcium phosphate (α-TCP, JCPDS no. 09−0348) and beta-tricalcium phosphate (β-TCP JCPDS no. 09−0169) were also identified in the coating. Undesired tetracalcium phosphate (TTCP) or calcium oxide (CaO) phases were not found in the coatings. Peaks related to Ag (JCPDS no. 87−0179) Ag_2O (JCPDS no. 19−1155) were found in HA-2Ag, HA-4Ag, and HA-6Ag indicating separate metallic Ag and Ag_2O phase incorporation. The peak intensity of (101) Ag_2O increased with increasing Ag_2O concentration in the coating.

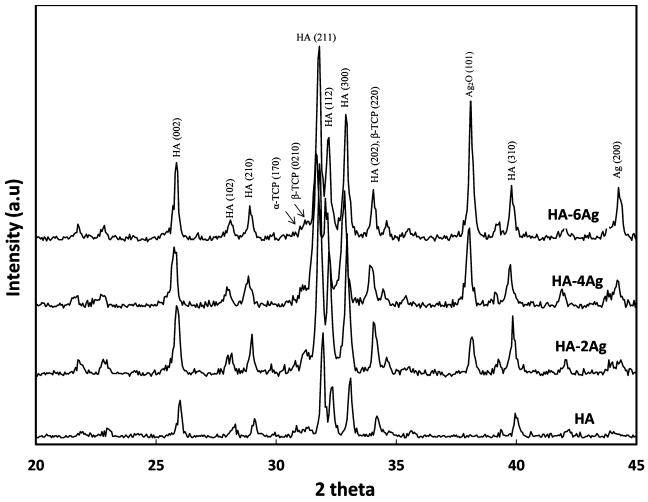

Figure 1. X-ray diffraction spectra of HA and Ag-doped HA coatings.

The FTIR spectra of the HA coatings are shown in Figure 2. Between 970 and 1190 cm^{-1}, antisymmetric (ν_3) P−O stretching

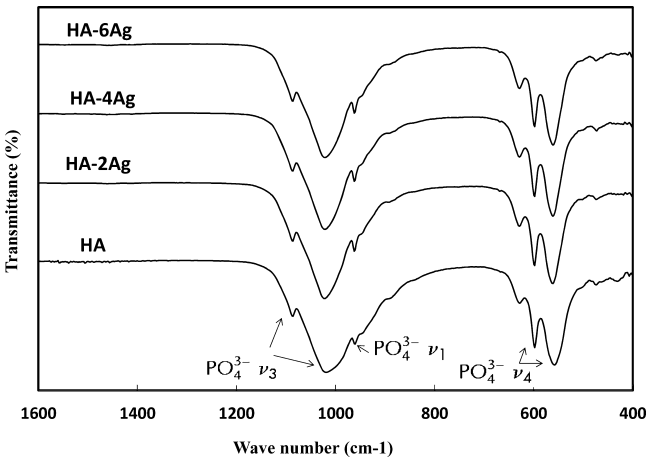

Figure 2. FTIR spectra of HA and Ag-doped HA coatings.

modes of the phosphate groups were found. The P−O (ν_1) symmetric stretching and antisymmetric (ν_4) bending modes were found at 960 cm^{-1} and in the region of 540 to 660 cm^{-1}, respectively. The peak positions and intensity were not affected by Ag doping.

3.2. Mechanical Properties. The tensile adhesive bond strength of the as sprayed coatings was determined according to ASTM C633. Bond strengths of HA, HA-2Ag, HA-4Ag, HA-6Ag were found to be 17.4 ± 2.9, 16.94 ± 0.41, 17.72 ± 1.78, and 15.75 ± 0.48 MPa. The failure surfaces were further digitally imaged in order to determine the failure mode. Figure 3 shows the

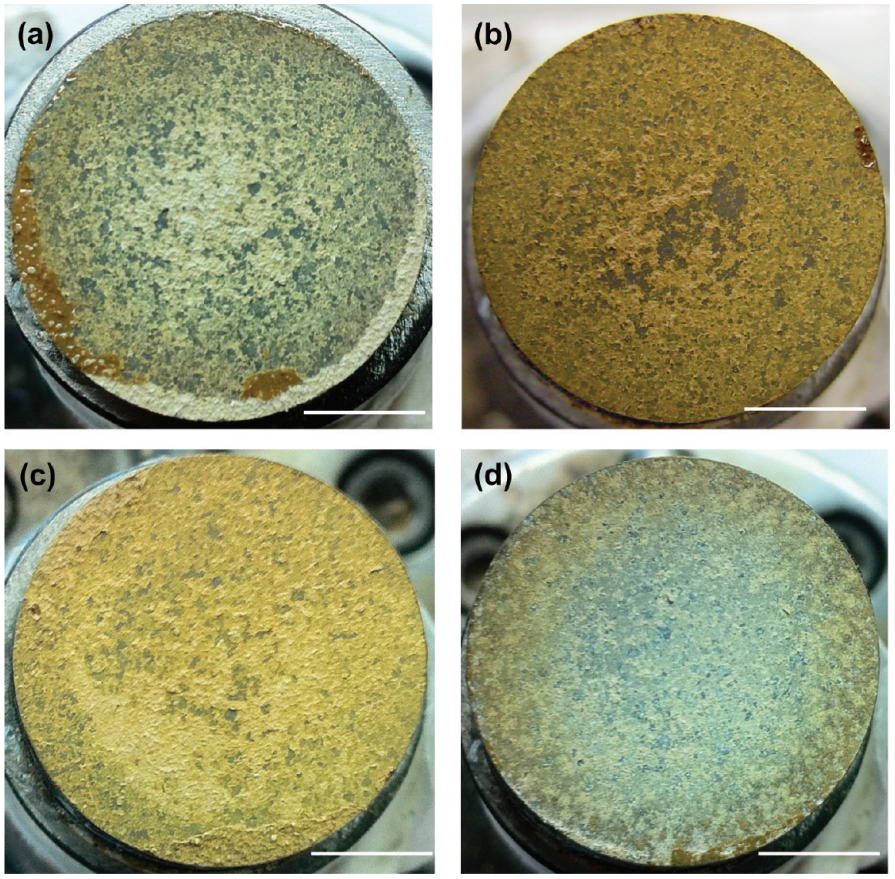

Figure 3. Images of the pull off area of (a) HA, (b) HA-2Ag, (c) HA-4Ag, and (d) HA-6Ag coatings. Coatings mostly indicated cohesive mode of failure (scale bar = 7.7 mm).

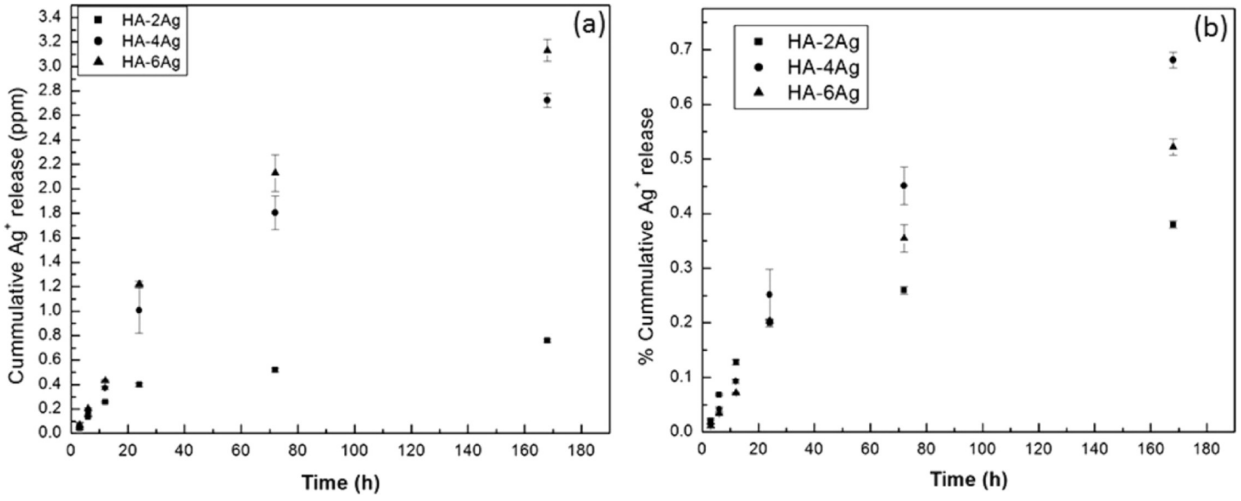

Figure 4. Release of Ag^+ from the coatings as a function of time (a) in parts per million (ppm) and (b) % release of the total Ag present in the coating.

failure surfaces of the coatings. Two different failure modes, adhesive (failure at coating−substrate interface) and cohesive (failure within the coating), were identified from the failure surfaces. All coatings showed cohesive mode of failure. Small amount of adhesive failure was noticed for HA-2Ag samples. None of the coatings showed pure adhesive failure, which indicated strong bonding between the coatings and the substrate.

3.3. Silver Release. Figure 4a shows the time-dependent cumulative silver release profile from HA-2Ag, HA-4Ag, and HA-6Ag coatings in PBS at 37 °C. Within first 6 h, Ag/Ag^+ release was independent of silver concentration in the coating and only released 200 ppb Ag/Ag^+. With increasing time, silver release increased in a concentration dependent manner and highest release was noticed for HA-6Ag at all-time points. Silver release form HA-2Ag was extremely low and cumulatively reached to 760 ppb even after 7 days of incubation in PBS. Silver release from all the coatings was within the minimum inhibitory concentration of Ag (6.25 ppm). Similar amount of

Ag/Ag^+ release has also been reported by many researchers.[22,34] The % release was also calculated based on the amount of silver present in the coating and is shown in Figure 4b. Cumulatively less than 1% total Ag released from the coatings after 7 days incubation in PBS.

3.4. In vitro Cell–Materials Interactions. *3.4.1. MTT Assay.* hFOB cell proliferation on undoped and Ag-doped HA coatings were determined by MTT assay. Figure 5 shows the comparative cell density on the coatings as a function of dopant concentration and culture time. At day 3, there was no significant difference in cell density among the Ag-doped and undoped HA coatings. With an increase in culture days, cell proliferated on all of the coatings with the exception of HA-6Ag. Cell proliferation was statistically significant at day 7 and 11 for HA and HA-4Ag coatings. In comparison, cell density on HA-2Ag coatings did not increase significantly at day 7 from day 3; however, it increased significantly at day 11 compared to day 3. For HA-6Ag, cell proliferation was not noticed at any culture days. At day 7, difference in cell density was statistically insignificant among HA, HA-2Ag, and HA-4Ag. By day 11, hFOB cells significantly proliferated on HA, HA-2Ag, and HA-4Ag; however, the difference among them was insignificant.

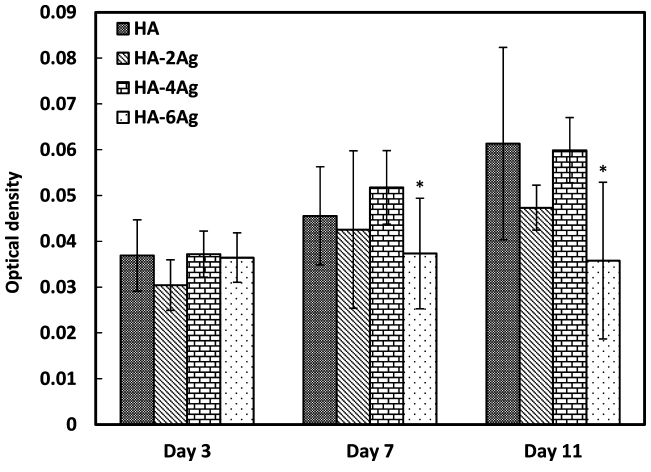

Figure 5. Optical density measurement illustrating hFOB cell proliferation on HA, HA-2Ag, HA-4Ag, and HA-6Ag after 3, 7, and 11 days of culture (*, $p < 0.05$, $n = 3$).

3.4.2. Cellular Morphology. Cellular attachment and growth of the hFOB cells on the doped and Ag-doped HA coatings were analyzed by FESEM. Figure 6 shows the cellular morphology and attachment behavior on the coated surfaces after 3 days of culture. As can be seen in Figure 6a, hFOB cells spontaneously attached to the HA coated surfaces with osteoblast phenotype and filopodia and pseudopodia extensions.[35] With an increase in Ag content in the coating, fewer cells were found to attach on the HA coatings, as shown in Figure 6c, d. Morphologically, adhered cells were similar on both HA and HA-4Ag with flattened morphology. On the HA-6Ag coating surfaces, few dead cells (indicated by solid white arrow) were found along with live cells, as shown in Figure 6d.

3.4.3. Alkaline Phosphatase Activity. ALP is an important protein expressed by differentiating osteoblast cells. We have evaluated the ALP expression as a differentiation marker for the hFOB cells cultured on HA, HA-2Ag, HA-4Ag, and HA-6Ag samples and are shown in Figure 7. In the fluorescence images, green and blue indicate proteins bound to ALP and nuclei, respectively. At day 5, hFOB cells showed positive immunostaining for ALP in all of the coated samples. Higher ALP activity was noticed on HA-4Ag and HA-6Ag samples after

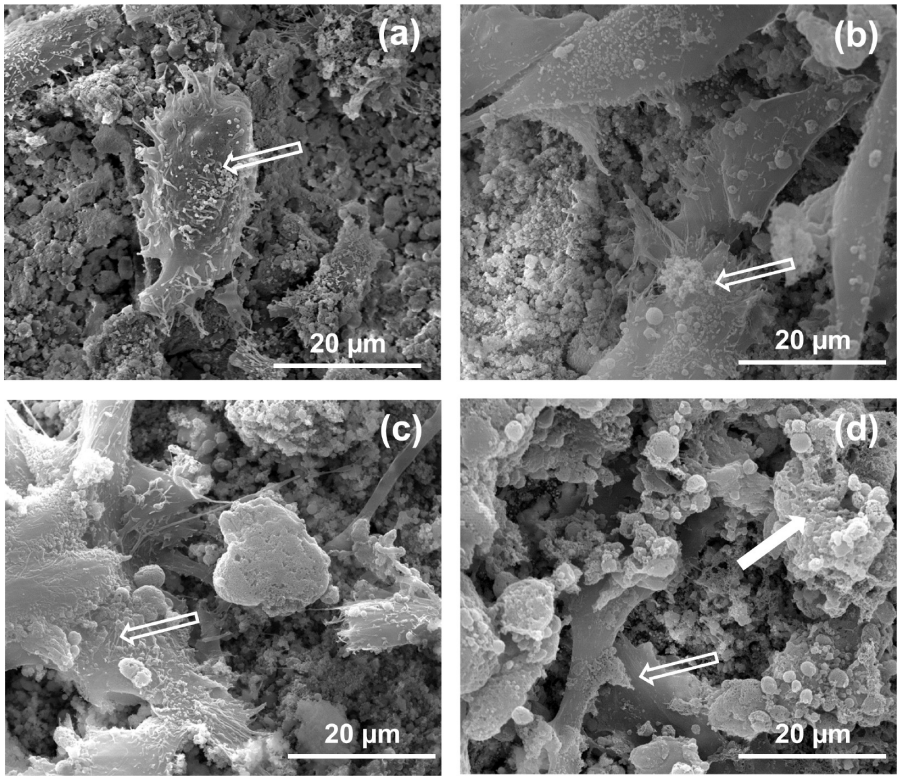

Figure 6. FESEM micrographs illustrating the hFOB cell morphology after 3 days of culture (a) HA, (b) HA-2Ag, (c) HA-4Ag, and (d) HA-6Ag. The open arrow indicates live cell and the solid arrow indicates dead cell.

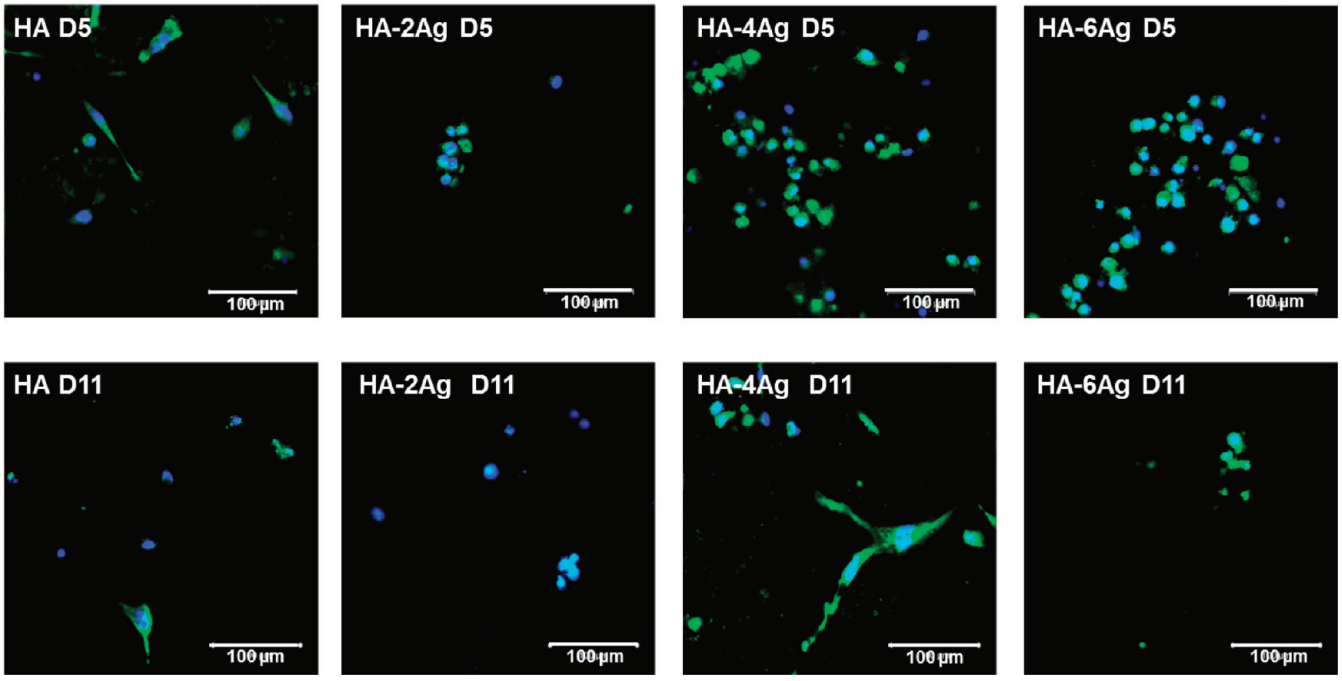

Figure 7. CLSM images of ALP expression in hFOB cells. The green fluorescence indicates antibody bound to ALP, blue fluorescence indicates PI bound to nucleus.

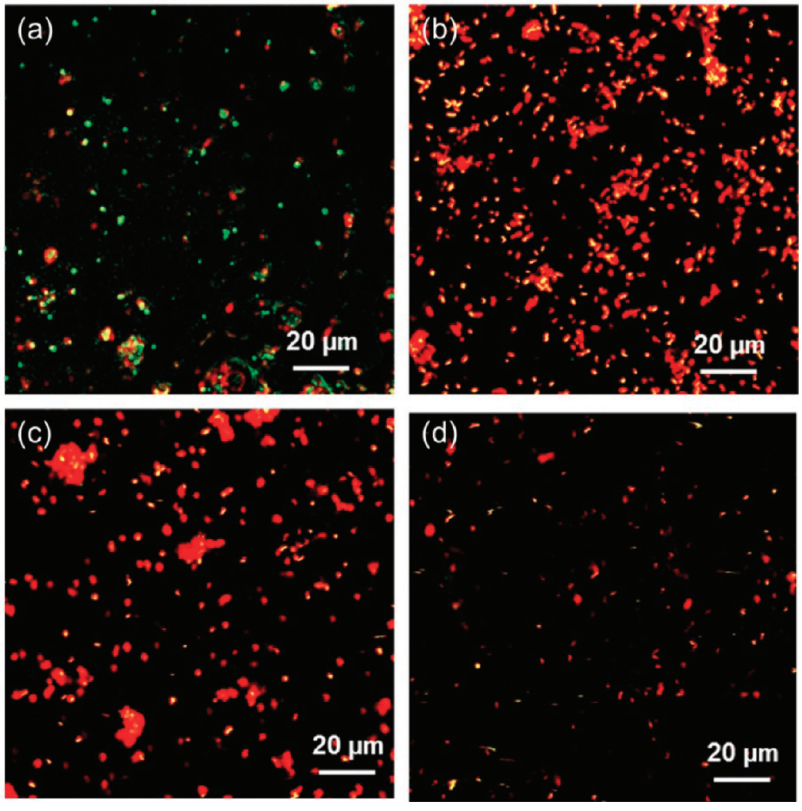

Figure 8. CLSM images showing viability of bacteria on (a) HA, (b) HA-2Ag, (c) HA-4Ag, and (d) HA-6Ag after 1 day of incubation. Red and green indicate dead and live bacteria, respectively.

5 days of cell culture. At day 11, ALP activity reduced in all of the coated samples.

3.5. Antimicrobial Activity. The efficacy of the Ag-doped HA coatings against the bacterial adhesion and colonization was verified by live/dead fluorescence staining and is shown in Figure 8. In the fluorescence images, green and red indicate live and dead bacteria, respectively. After 24 h of culture, large number of live bacteria was found on pure HA coatings, as shown in Figure 8a. In Figure 8b, large number of adhered bacteria was noticed on HA-2Ag coating surfaces. However,

majority of the single or colonized bacteria was found dead with only few of them surviving on the surface. On the HA-4Ag samples, visibly fewer bacteria were found that were mostly dead, as shown in Figure 8c. Very few single or colonized bacteria were found to adhere on the HA-6Ag samples. As noticed in Figure 8d, live bacteria were scarce on HA-6Ag samples.

4. DISCUSSION

In the present study, we have evaluated the Ag concentration-dependent antimicrobial activity of plasma-sprayed HA coatings. To maintain the bioactivity of HA coatings, we also evaluated cytocompatibility using hFOB cells.

Some of the major challenges of plasma-sprayed HA coatings are phase decomposition and amorphous phase formation. Because of the very high processing temperature (≥10 000 °C), plasma-sprayed HA coatings generally contain secondary phases such as α/β-TCP or CaO/TTCP as undesirable phases. However, in the present study, we have used a specially designed supersonic nozzle, which significantly contributed to the reduced phase decomposition and amorphous phase formation.[34,35] In supersonic plasma nozzle, HA particles are discharged in the lower region of the plasma, where the temperature is low and at a velocity of 510 m/s.[34] Thus the phase decomposition is restricted because of the reduced exposure of HA particles to the plasma. The sharp and distinct HA peaks indicate that the coatings are relatively phase pure and crystalline in nature. Incorporation of Ag is found to have insignificant effect on phase decomposition and crystallinity of the coatings, which can be attributed to the plasma spray processing. In plasma spray, individual particles travel through the plasma region where they partially melt and then forced to the substrate to form the coating.[37] Being comparable in particle size, Ag-doped and undoped HA particles experience similar heat treatment in the plasma and therefore shows similar behavior in terms of phase decomposition and amorphous phase formation.[38] The XRD results show slight peak shifts in the 2θ values for samples that contained Ag_2O indicating incorporation of silver ions into the HA lattice structure, likely as a substitution for Ca^{2+}.[39] The separate Ag_2O deposits within the coating are further verified by visual inspection, noting the dark brown color of the coatings. The sharp and distinct phosphate bands in the FTIR spectra of Ag-doped and undoped HA coatings also confirm the high crystallinity of the coatings. In our previous works, we have demonstrated that the crystalline HA coatings can be characterized by sharp and distinct FTIR spectra.[34,35]

Similar to chemical properties, adhesive bond strength of the plasm-sprayed HA coatings are not significantly influenced by Ag doping. Chemistry of the coatings does not alter the adhesive strength of the coatings because of the fact that plasma-sprayed HA coatings are mechanically bonded to the substrate. The similar sized HA and Ag-doped HA particles goes through the same coating formation process, as explained before and results in similar adhesive strength. The failure surface analysis of the HA coatings indicate that the primary mode of failure is cohesive (interlayer failure). Although some adhesive failure is noticed in HA-2Ag coatings, the primary mode of failure is cohesive, which indicates that the coating is strongly bonded with the Ti substrate. As indicated in other literatures, the cohesive mode of failure indicates a stronger bonding of the coatings with the substrate and incomplete failure even at high loads.[39]

The performance of a hydroxyapatite-coated metallic implants are primarily dictated not only by its physicochemical and mechanical properties but also its biological activity. The ability of the implant surface to provide the necessary support for osteoblastic synthesis of new bone is very important. Along with that, the implant needs to provide the host defense for bacterial adhesion for a successful implant integration and survivability. HA is known as a bioactive ceramic and Ag has long been studied as an antimicrobial agent and successfully used in the biomedical prosthesis and surgical instruments.[23−25,33] The antimicrobial activity of Ag can be explained in many ways. It has been reported that Ag ions can damage the bacterial outer membrane, leading to cell death.[25,40] The silver ion can also bind to sulphydryl groups of the respiratory enzymes, the nucleic acids, and ribosomal subunit proteins resulting in inhibiting the normal cell functions and cell death.[32,41−43] Moreover, Ag can create hydroxyl radicals (·OH) and superoxide anions (O_2^-) by photocatalytic reactions, which can lead to protein inactivation and eventual cell apoptosis.[25,44] Such multidimensional influence of Ag^+ on bacteria makes it quite effective for a variety of species including both gram negative and gram positive bacteria. Our present results have indicated that all the Ag-doped HA coatings are successful in restricting bacterial adhesion. The lowest amount of bacterial adhesion on HA-6Ag samples can be attributed to the higher amount of Ag in the coating.

In our previous works, we have shown that presence of Ag on the surface of LENS processed TCP coating and silver-coated titania nanotubes on the surface of Ti substrates can significantly enhance its antimicrobial activity.[32,33] However, for open wounds, prevention of stage II and III infections will require having a continual defense against bacterial adhesion. In our present work, Ag has been structurally incorporated into the coating in the form of Ag^+ substitution into the HA lattice structure as well as metallic Ag and Ag_2O deposits within the coating. The Ag^+ release profile confirms that less than 1% of the total Ag is coming out of the coating, whereas 99% of Ag is staying within the coating. During the first 2 years after total knee arthroplasty, infections are counted as the second most common cause for revision surgery after instability.[45] Perioperative broad spectrum antibiotic treatments are not effective in preventing biofilm formation on the surface of the implant. Due to the slow breakdown of HA in vivo and the resulting slow Ag release from the coating, the surface of the implant where biofilms are most likely to form can remain protected for extensive periods of time. Although a study of 6 months and higher can demonstrate the true long-term efficacy of these Ag doped HA coatings against bacterial adhesion, with our present results we conclude that the large amount of Ag incorporated within the HA coatings will maintain its antimicrobial efficacy with time.

Although Ag is extensively used as antimicrobial agents, concerns regarding its cytocompatibility have been raised.[23,31−33,46] Our present results indicate that at higher concentrations, Ag can induce toxicity leading to restricted cell proliferation and cell death. The MTT assay shows that the hFOB cells fail to proliferate on HA-6Ag coating where the cellular morphology indicates cell death. It has been reported that high concentration of Ag can result in reduction of intracellular adenosine triphosphate (ATP) content and lead to cell death.[41] In the present work, higher Ag content samples also shows reduction in cell density compared to pure HA coatings; however, the difference was not statistically significant.

Similar results has also been reported in a recent article where it has been explained that static condition of the in vitro culture model results in accumulation of Ag in the media and results in cell death.[23] In physiological conditions, Ag will circulate in blood, where intestine absorbs a small quantity of it while a majority is excreted by liver.[47] The immunofluorescence images indicate that lower concentrations of Ag do not affect the ALP activity of osteoblast cells. Similar findings have been reported by Song et al., where Ag-doped calcium phosphate coating is found to have minimal effects on ALP activity after 7 days of culture.[26] The ALP activity reduced at day 11 from day 5, which can be due to a cumulative effect of Ag accumulation and not necessarily due to cytotoxicity. In comparison to cytocompatibility study, the antimicrobial study was done with a much higher sample to media ratio (28 mL media/sample for antimicrobial study compared to 1 mL/sample in cytocompatibility study) and with constant stirring. Hence, the antimicrobial study is more dynamic, which represents true antimicrobial activity of the surface and does not represent reduction in bacterial adhesion due to Ag accumulation. Although Ag has shown to have toxic effects at higher concentrations, studies have indicated that with proper amount of Ag incorporation, biomaterials can enhance osteoblast proliferation.[32,48−50] Ag-doped beta-TCP disks not only found to facilitate osteoblast precursor cell (OPC-1) proliferation but also assist in apatite deposition.[51] It has been reported that 2.05 ± 0.55 wt % Ag-doped HA coatings significantly reduced the bacterial adhesion without any significant cytoxicity.[42] Therefore, it is vitally important to incorporate optimum amount of Ag in hydroxyapatite coatings to have sustained antimicrobial property while minimizing cytotoxicity. Our results suggest that the plasma-sprayed HA coatings doped with both 2 and 4 wt % Ag have excellent antimicrobial properties while minimizing cell damage.

5. CONCLUSIONS

We have demonstrated that Ag can be successfully incorporated in plasma sprayed HA coating. The specially designed supersonic plasma nozzle helped in retaining the phase purity and crystallinity of the coating where the physicochemical properties were not significantly affected by Ag incorporation. An adhesive strength greater than 15 MPa ensured mechanical integrity of the coatings. Incorporation of Ag in the HA coating significantly reduced *P. Aeruginosa* (PAO1) adhesion on the coating surface in a concentration dependent manner. Although 6 wt % Ag incorporation showed highest antimicrobial properties, it reduced hFOB cell proliferation as well. A balance between good hFOB cell-materials interactions and antimicrobial property was achieved with 2 and 4 wt % Ag in the HA coating. It is also predicted that the incorporation of Ag within the structure of the plasma-sprayed HA coating, rather than on the coating surface, will provide long-term host defense against bacterial adhesion. In summary, an optimum amount of structurally incorporated Ag in the plasma-sprayed HA coatings has the potential to reduce long-term bacterial adhesion to the implant surface while maintaining healthy osteoblast cellular activity.

AUTHOR INFORMATION

Corresponding Author

*Tel: 509-335-7461. Fax: 509-335-4662. E-mail: sbose@wsu.edu.

Notes

The authors declare no competing financial interest.

ACKNOWLEDGMENTS

The authors acknowledge financial support from the National Institute of Health (N1H-RO1-EB-007351). The authors also like to acknowledge the financial support from the Office of Naval Research and the W. M. Keck Foundation to establish a Biomedical Materials Research Laboratory at WSU. We are also grateful to the Franceschi Microscopy and Imaging Center of Washington State University for the use of their facilities and staff assistance.

REFERENCES

(1) Yang, Y.; Kim, K. H.; Ong, J. L. *Biomaterials* **2005**, *26*, 327−337.
(2) Roy, M.; Vamsi, K. B.; Bandyopadhyay, A.; Bose, S. *Acta. Biomater.* **2008**, *4*, 324−333.
(3) Roy, M.; Bandyopadhyay, A.; Bose, S. *J. Am. Ceram. Soc.* **2008**, *91*, 3517−3521.
(4) Narayanan, R.; Seshadri, S. K.; Kwon, T. Y.; Kim, K. H. *J. Biomed. Mater. Res. Part B Appl. Biomater.* **2008**, *85B*, 279−99.
(5) Roy, M.; Balla, V. K.; Bandyopadhyay, A.; Bose, S. *Acta. Biomater.* **2011**, *7*, 866−873.
(6) Sun, L.; Berndt, C. C.; Gross, K. A.; Kucuk, A. *J. Biomed. Mater. Res.* **2001**, *58*, 570−592.
(7) Mäkelä, K. T.; Eskelinen, A.; Pulkkinen, P.; Paavolainen, P.; Remes, V. *J. Bone Joint Surg. Am.* **2008**, *90*, 2160−2170.
(8) Eskelinen, A.; Paavolainen, P.; Helenius, I.; Pulkkinen, P.; Remes, V. *Acta Orthop.* **2006**, *77*, 853−865.
(9) Chambers, B.; Clair, S. F.; Froimson, M. I. *J. Arthroplasty* **2007**, *22* (s1), 71−74.
(10) Gabbar, O. A.; Rajan, R. A.; Londhe, S.; dyde, I. D. *J. Arthroplasty* **2008**, *23*, 413−417.
(11) Shah, N. N.; Edge, A. J.; Clark, D. W. *J. Bone Joint Surg. Br.* **2009**, *91B*, 865−869.
(12) Gulotta, L. V.; Baldini, A.; Foote, K.; Lyman, S.; Nestor, B. J. *HSS J.* **2008**, *4*, 55−61.
(13) Trikha, S. P.; Singh, S.; Raynham, O. W.; Lewis, J. C.; Mitchell, P. A.; Edge, A. *J. Bone Joint Surg. Br.* **2005**, *87B*, 1055−1060.
(14) Raman, R.; Kamath, R. P.; Parikh, A.; Angus, P. D. *J. Bone Joint Surg. Br.* **2005**, *87B*, 1061−1067.
(15) Lie, S. A.; Havelin, L. I.; Furnes, O. N.; Engesæter, L. B.; Vollset, S. E *J. Bone Joint Surg. Br.* **2004**, *86B*, 504−509.
(16) Jafari, S. M.; Coyle, C.; Mortazavi, S. M. J.; Sharkey, P. F.; Parvizi. *J. Clin. Orthop. Relat. Res.* **2010**, *468*, 2046−2051.
(17) Darwiche, H.; Barsoum, W. K.; Klika, A.; Krebs, V. E.; Molloy, R. *Clin. Orthop. Relat. Res.* **2010**, *468*, 2392−2396.
(18) Geerdink, C. H.; Schaafsma, J.; Meyers, W. G. M.; Grimm, B.; Tonino, A. J. *J. Arthroplasty* **2007**, *22*, 369−376.
(19) Coventry, M. B. *Orthop. Clin. North. Am.* **1975**, *6*, 991−1003.
(20) Tsukayama, D. T.; Estrada, R.; Gustilo, R. B. *J. Bone Joint Surg. Am.* **1996**, *78*, 512−523.
(21) Senthi, S.; Munro, J. T.; Pitto, R. P. *Int. Orthop.* **2011**, *35*, 253−260.
(22) Zhao, L.; Wang, H.; Huo, K.; Cui, L.; Zhang, W.; Ni, H.; Zhang, Y.; Wu, Z.; Chu, P. K. *Biomaterials* **2011**, *32*, 5706−5716.
(23) Ewald, A.; Hösel, D.; Patel, S.; Grover, L. M.; Barralet, J. E.; Gbureck, U. *Acta Biomater.* **2011**, *7*, 4064−4070.
(24) Matsumoto, N.; Sato, K.; Yoshida, K.; Hashimoto, K.; Toda, Y. *Acta Biomater.* **2009**, *5*, 3157−3164.
(25) Song, W. H.; Ryu, H. S.; Hong, S. H. *J. Biomed. Mater. Res.* **2009**, *88A*, 246−254.
(26) Niikura, T.; Tsujimoto, K.; Yoshiya, S.; Tadokoro, K.; Kurosaka, M.; Shiba, R. *Orthopedics* **2007**, *30*, 320−321.
(27) Stallmann, H. P.; Faber, C.; Bronckers, A. L. J. J.; Amerongen, A, V, N.; Wuisman, P. I. *J. Antimicrob. Chemother.* **2004**, *54*, 472−476.

(28) Ramesh, N.; Kumar, K. R.; Kumar, T. S. S.; Sunder, M.; Victor, S. P. *Trends. Biomater. Artif. Organs* **2005**, *18*, 213−218.
(29) Paul, W.; Sharma, C. P. *J. Mater. Sci. Lett.* **1995**, *14*, 1792−1794.
(30) Jain, J.; Arora, S.; Rajwade, J. M.; Omray, P.; Khandelwal, S.; Paknikar, K. M. *Mol. Pharm.* **2009**, *6*, 1388−1401.
(31) Ramstedt, M.; Ekstrand-Hammarstrom, B.; Shchukarev, A. V.; Bucht, A.; Osterlund, L.; Welch, M.; Wilhelm, T. S. H. *Biomaterials* **2009**, *30*, 1524−1531.
(32) Roy, M.; Bandyopadhyay, A.; Bose, S. *Mater. Sci. Eng., C* **2009**, *29*, 1965−1968.
(33) Das, K.; Bose, S.; Bandyopadhyay, A.; Karandikar, B.; Gibbins, B. L. *J. Biomed. Mater. Res. B* **2008**, *87B*, 455−460.
(34) Roy, M.; Bandyopadhyay, A.; Bose, S. *J. Biomed. Mater. Res., Part B* **2011**, *99B*, 258−265.
(35) Roy, M.; Bandyopadhyay, A.; Bose, S. *Surf. Coat. Technol.* **2011**, *205*, 2785−2792.
(36) Lewandowski, Z., Beyenal, H. *Fundamentals of Biofilm Research*; CRC Press: London, 2007; pp 410−418.
(37) Sun, L.; Berndt, C. C.; Grey, C. P. *Mater. Sci. Eng., A.* **2003**, *360*, 70−84.
(38) Khor, K. A.; Cheang, P. *J. Mater. Process. Technol.* **1997**, *63*, 271−276.
(39) Tang, Y.; Chappell, H. F.; Dove, M. T.; Reeder, R. J.; Lee, Y. J. *Biomaterials* **2009**, *30*, 2864−2872.
(40) Bai, X.; More, K.; Rouleau, C. M.; Rabiei, A. *Acta. Biomater.* **2010**, *6*, 2264−2273.
(41) Amro, N. A.; Kotra, L. P.; Wadu-Mesthrige, K.; Bulychev, A.; Mobashery, S.; Liu, G. *Langmuir* **2000**, *16*, 2789−2796.
(42) Chen, W.; Liu, Y.; Courtney, H. S.; Bettenga, M.; Agrawal, C. M.; Bumgardner, J. D.; Ong, J. L. *Biomaterials* **2006**, *27*, 5512−5517.
(43) Das, K.; Bose, S.; Bandyopadhyay, A.; Karandikar, B.; Gibbins, B. L. *J. Biomed. Mat. Res., Part B* **2008**, *87B*, 455−460.
(44) Sunada, K.; Watanabe, T.; Hashimoto, K. *J. Photochem. Photobiol. A* **2003**, *156*, 227−33.
(45) Gioe, T. J.; Killeen, K. K.; Grimm, K.; Mehle, S.; Scheltema, K. *Clin. Orthop. Relat. Res.* **2004**, *428*, 100−106.
(46) Lischer, S.; Körner, E.; Balazs, D. J.; Shen, D.; Wick, P.; Grieder, K.; Haas, D.; Heuberger, M.; Hegemann, D. *J. R. Soc. Interface* **2011**, *8*, 1019−1030.
(47) Clement, J. L.; Jarrett, P. S. *Metal-Based Drugs* **1994**, *1*, 467−482.
(48) Hardes, J.; Ahrens, H.; Gebert, C.; Streitbuerger, A.; Buerger, H.; Erren, M.; Gunsel, A.; Wedemeyer, C.; Saxler, G.; Winkelmann, W.; Gosheger, G. *Biomaterials* **2007**, *28*, 2869−2875.
(49) Bosetti, M.; Massè, A.; Tobin, E.; Cannas, M. *Biomaterials* **2002**, *23*, 887−892.
(50) Alt, V.; Bechert, T.; Steinrücke, P.; Wagener, M.; Seidel, P.; Dingeldein, E.; Domann, E.; Schnettler, R. *Biomaterials* **2004**, *25*, 4383−4391.
(51) Seeley, Z.; Bandyopadhyay, A.; Bose, S. *J. Biomed. Mater. Res., Part A* **2007**, *82A*, 113−121.